Influence of illumination on the quantum mobility of a two-dimensional electron gas in Si δ-doped GaAs/$In_{0.15}Ga_{0.85}As$ quantum wells

2003 J. Phys.: Condens. Matter 15 121

(http://iopscience.iop.org/0953-8984/15/2/312)

INSTITUTE OF PHYSICS PUBLISHING JOURNAL OF PHYSICS: CONDENSED MATTER

J. Phys.: Condens. Matter **15** (2003) 121–132 PII: S0953-8984(03)39522-0

Influence of illumination on the quantum mobility of a two-dimensional electron gas in Si δ-doped GaAs/$In_{0.15}Ga_{0.85}As$ quantum wells

A Cavalheiro[1], E C F da Silva[2], A A Quivy[2], E K Takahashi[1], S Martini[2], M J da Silva[2], E A Meneses[3] and J R Leite[2]

[1] Departamento de Ciências Físicas da Universidade Federal de Uberlândia, CP 595, 38400-902 Uberlândia, MG, Brazil
[2] Instituto de Física da Universidade de São Paulo, Laboratório de Novos Materiais Semicondutores, CP 66318, 05315-970 São Paulo, SP, Brazil
[3] Instituto de Física Gleb Wataghin, Universidade Estadual de Campinas, CP 6165, 17083-970 Campinas, SP, Brazil

Received 16 July 2002, in final form 5 November 2002
Published 20 December 2002
Online at stacks.iop.org/JPhysCM/15/121

Abstract

A series of GaAs/InGaAs quantum wells with a silicon δ-doped layer in the top barrier was investigated by Shubnikov–de Haas measurements as a function of the illumination time of the samples. During the illumination process strong modifications of the electronic density and the quantum mobility of each occupied subband were observed. Based on self-consistent calculations, the dominant mechanism which caused the changes in the subband quantum mobilities with illumination was elucidated.

1. Introduction

In recent years, there has been a revival of interest in the transport properties of a two-dimensional electron gas (2DEG) [1]. This has been largely motivated by the experimental progress in controlled preparation of nanostructured semiconductor systems and by the practical importance of high-mobility heterostructures, in which impurities are separated from the 2DEG by a wide spacer. In particular, considerable experimental and theoretical effort has been made to understand the electrical and optical properties of $In_xGa_{1-x}As$-based heterostructures since it was demonstrated that they could be very important to the development of high-performance devices [2]. The device performance in high-electron-mobility transistors (HEMTs) can be further improved by using delta doping (δ doping) instead of the conventional modulation bulk doping technique [3]. Particularly, when an n-type δ-doped layer is placed in the barrier region close to a quantum well (QW), the electrons released by the dopants are partially transferred from the δ-doped layer to the QW to keep the Fermi level constant over the entire structure. In such a δ-doped modulation QW (δ-MDQW), a 2DEG of very high

mobility can be achieved at the QW interface because of the physical separation of electrons from the ionized donors in the barrier [4, 5].

Several reports on the transport properties on Si δ-doped GaAs/InGaAs/GaAs QWs have been published recently and the transfer of electrons from one channel to the other one, and the persistent photoconductivity effect (PPC) observed in these structures, have been the subject of main interest [6–10]. Two parameters are extremely important to investigate the origin of the PPC effect and the transfer of carriers between QWs: the total free-electron concentration and the carrier mobility. By analysing the different oscillation periods contained in the SdH curves (using an FFT algorithm), it is possible to obtain the carrier density of the individual subbands and, consequently, the total free-electron concentration. However, the electron mobility of each subband is a parameter that, in contrast to the electron density, is not so easily accessible because it requires a more complex processing of the data. As far as carrier mobility is concerned, most of the work performed so far obtained this parameter using Hall-effect measurements that only provide an average value of the mobility of the whole system. Moreover, in our previous work [10], we clearly demonstrate that a systematic study of the transport properties as a function of illumination time is very important and can avoid misleading interpretation of the data. So, in the present work, using the illumination as a tool, we were able to follow, in an accurate way, the evolution of the electronic density and the quantum mobility of each subband of the several Si δ-doped GaAs/InGaAs QWs. We compare the experimental data obtained by our SdH measurements with the results of self-consistent electronic-structure calculations, which include the light-induced modifications of the electronic wavefunctions due to the photoexcitation. Our theoretical data also confirmed that deep traps and surface states are responsible for the PPC effect observed in our samples.

2. Experimental details

All the samples designed for this study were grown on an MBE system on top of an epi-ready GaAs(001) substrate and consist of a 1 μm-thick GaAs buffer layer followed by a 10 $\times$ $(AlAs)_5(GaAs)_{10}$ superlattice, a 1000 Å-thick GaAs back barrier, a 150 Å-wide $In_{0.15}Ga_{0.85}As$ QW, a D-thick GaAs spacer, a silicon δ-doped layer with a nominal Si concentration $N_{Si} = 4.0 \times 10^{12}$ cm^{-2} and a GaAs top barrier of 500 Å. The top 100 Å thick GaAs cap layer was doped to $n_{cap} = 10^{17}$ cm^{-3}. Details of sample growth are described in [10]. Three samples were grown with a different value (D) of the thickness spacer layer and were designated as D20, D40 and D100. The number indicates the thickness (Å) of the spacer layer.

The Shubnikov–de Haas (SdH) measurements were carried out using a standard van der Pauw configuration, a 10 μA dc current and the following conditions: the first measurement was performed just after cooling the sample down in the dark. Next, the sample was illuminated for a short period of time and a second SdH measurement was performed in the dark. The same procedure (but with a longer and longer period of illumination followed by the SdH measurement in the dark) was applied several times until no significant change of the data could be observed. The sample was illuminated by a light-emitting diode (LED) whose photon energy ($\sim$1.74 eV) was larger than the bandgap energy of the GaAs material at 1.5 K ($\sim$1.52 eV).

As described in an earlier paper [10], in order to determine the electronic density and the quantum mobility of the occupied subbands, our magnetoresistance traces (R_{xx}) were numerically differentiated, expressed as a function of the reciprocal magnetic field ($1/B$), and multiplied by a smooth window function (the Hanning function) before computing their fast Fourier transform (FFT). The quantum mobility of a specific subband was determined by the logarithmic dependence of the maximum amplitude of the FFT peak plotted against

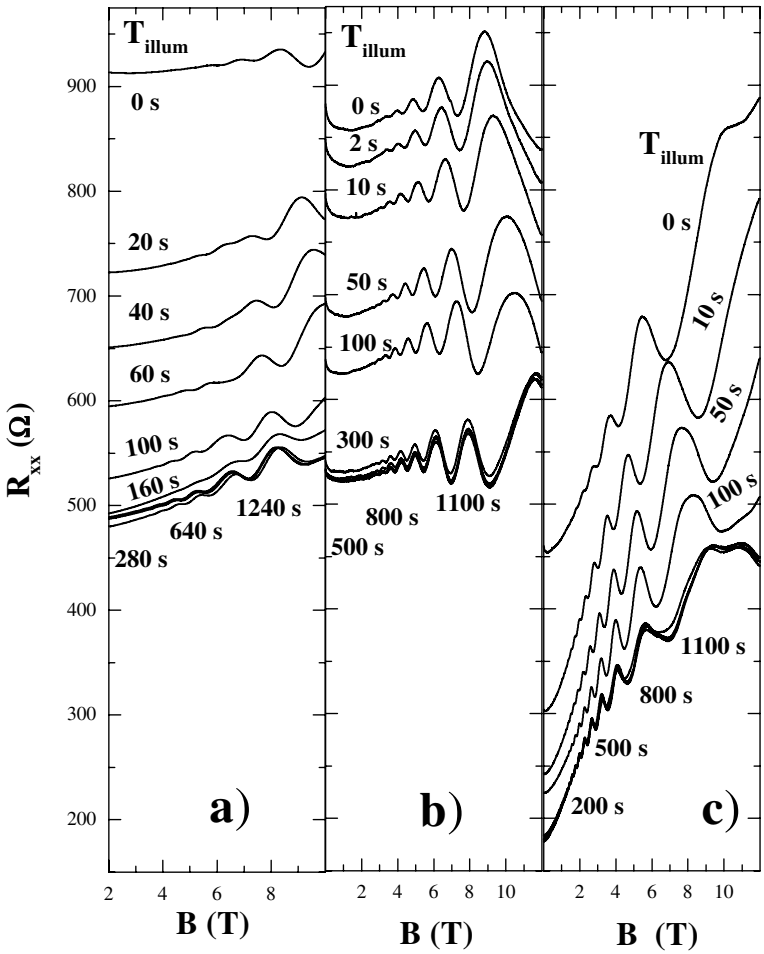

Figure 1. Magnetoresistance (R_{xx}) of n-type δ-MDQWs with similar architectures but with different spacer thicknesses: (a) 20 Å; (b) 40 Åand (c) 100 Å. For all samples, the curves indicated by $T_{illum} = 0$ s were recorded just after cooling down the sample in the dark; the other curves were recorded in the dark but after subsequent illumination periods, as indicated.

$1/B$ [11, 12]. In these conditions, the slope of the straight line through the data is equal to π/μ_i ($i = 1, 2, 3 \ldots$). The electron subband densities n_i were related to the frequencies ν_i of the SdH oscillations by the expression $n_i = 2e\nu_i/h$ where e is the electronic charge and h is Planck's constant. The total free-electron density n_s was determined by summing the individual electron density of all the observed subbands, $n_s = \sum_i n_i$.

3. Experimental results

Figure 1 shows the results of the SdH measurements for the different illumination time periods (T_{illum}) for all the samples analysed here. We can see that R_{xx} decreases gradually as a function of the illumination time and reaches a saturated stage for sufficiently long illumination times. This decrease of the magnetoresistance with illumination is a consequence of the long-lifetime photoconductivity effect observed in all samples analysed here. For example, after the measurement performed at $T_{illum} = 1240$ s, sample D20 was kept in the dark, inside the

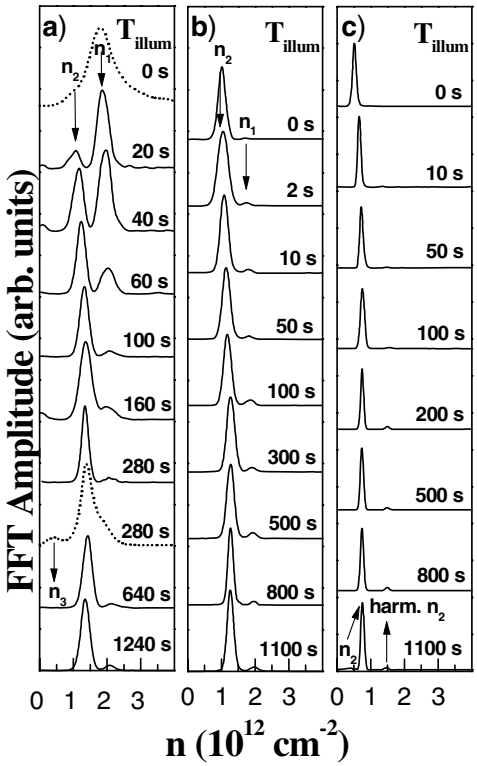

Figure 2. FFT spectra of the traces shown in figure 1, obtained after windowing the magnetoresistance curves with the Hanning function. The dashed curves in (a) were obtained when a simple FFT procedure was used to process the magnetoresistance data. The spectra have been vertically displaced for clarity.

cryostat, for 27 h. After that time, an SdH measurement was performed in the dark and the recorded magnetoresistance showed the same trace as the one obtained for $T_{illum} = 1240$ s indicating a lifetime of 27 h, at least.

The SdH oscillations shown in figure 1 indicate the presence of a 2DEG in the active region (considered here as composed by the δ-doped QW and the InGaAs QW) of all samples, even before their exposure to any illumination (curves indicated by $T_{illum} = 0$ s). In figure 2 we show the data obtained after the FFT processing of the respective SdH traces shown in figure 1. Two occupied subbands (n_1 and n_2) were found in the FFT spectra of the *windowed* magnetoresistance data for samples D20 and D40 while only one (n_2) was detected for sample D100. The small peak observed at $\approx 1.5 \times 10^{12}$ cm^{-2} in figure 2(c) does not correspond to any occupied subband of sample D100 since this peak is a harmonic of that observed at $\approx 0.75 \times 10^{12}$ cm^{-2}. A third subband was also clearly observed for sample D20 for $T_{illum} \geqslant 280$ s when a simple FFT procedure was used to process the magnetoresistance data[4] (dashed curve in figure 2(a)). The FFT of the windowed curves generally provides better-resolved data at the expense of the intensity of the peaks related to the less occupied subbands. This is the reason why the third subband was not observed in the FFT spectra obtained after windowing the magnetoresistance traces of sample D20 for $T_{illum} \geqslant 280$ s.

[4] A detailed presentation and discussion of the magnetoresistance data related to sample D20 is given in the recent paper of [10].

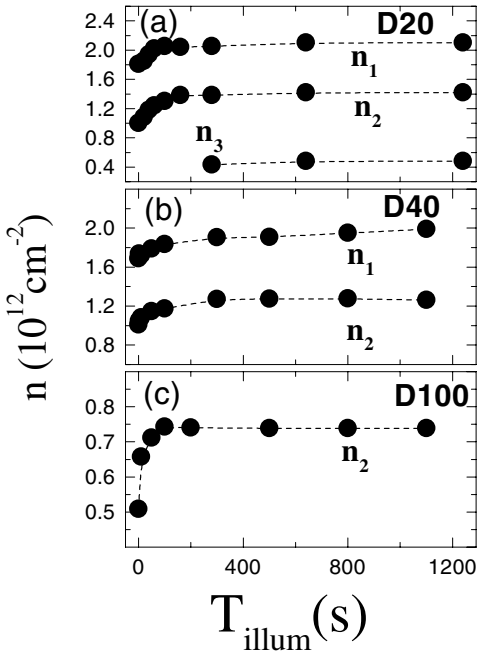

Figure 3. Electron density of the occupied subbands as a function of the illumination time for the samples: (a) D20; (b) D40 and (c) D100. The dashed lines connecting the peaks are a guide to the eyes.

The electron density of each subband extracted from the FFT spectra of the magnetoresistance data is presented in figure 3 as a function of the illumination time. This figure clearly evidences the PPC effect observed in all samples which manifests itself as an increase of the electron density of the occupied subbands and as a saturation for large illumination periods. For sample D20, at $T_{illum} = 0$ s, there are two occupied subbbands with electron densities $n_1 = 1.81 \times 10^{12}$ cm^{-2} and $n_2 = 1.00 \times 10^{12}$ cm^{-2}. Therefore, the total electron concentration of the 2DEG before exposure of sample D20 to any illumination is $n_s = 2.81 \times 10^{12}$ cm^{-2}. A further illumination process increases the population of the occupied subbands, and at $T_{illum} = 280$ s a third subband with $n_3 = 0.43 \times 10^{12}$ cm^{-2} was observed using the simple FFT procedure (dashed curve in figure 2(a)). In the saturated stage we found $n_1 = 2.10 \times 10^{12}$ cm^{-2}, $n_2 = 1.42 \times 10^{12}$ cm^{-2} and $n_3 = 0.48 \times 10^{12}$ cm^{-2} which gives $n_s = 4.00 \times 10^{12}$ cm^{-2}, a value corresponding to the nominal silicon concentration $N_{\mathrm{Si}} = 4.0 \times 10^{12}$ cm^{-2}. For sample D40 we found $n_1 = 1.69 \times 10^{12}$ cm^{-2} and $n_2 = 1.01 \times 10^{12}$ cm^{-2} ($n_s = 2.70 \times 10^{12}$ cm^{-2}) before exposure of the sample to any illumination and $n_1 = 1.99 \times 10^{12}$ cm^{-2} and $n_2 = 1.26 \times 10^{12}$ cm^{-2} ($n_s = 3.25 \times 10^{12}$ cm^{-2}) after the illumination process. For sample D100, only one subband was detected with an electron density $n_s = n_2 = 0.51 \times 10^{12}$ cm^{-2} before the illumination process. In the final process of illumination, we observed an increase of 0.23×10^{12} cm^{-2} in the occupation of this subband.

For the samples analysed here, the quantum mobility of each subband was determined using the procedure presented in section 2 and the results are shown in figure 4. For sample D20, the mobility (μ_1) of the first subband (the fundamental electronic state) decreases whereas the mobility of the first excited electronic state (μ_2) increases with illumination time. Our results

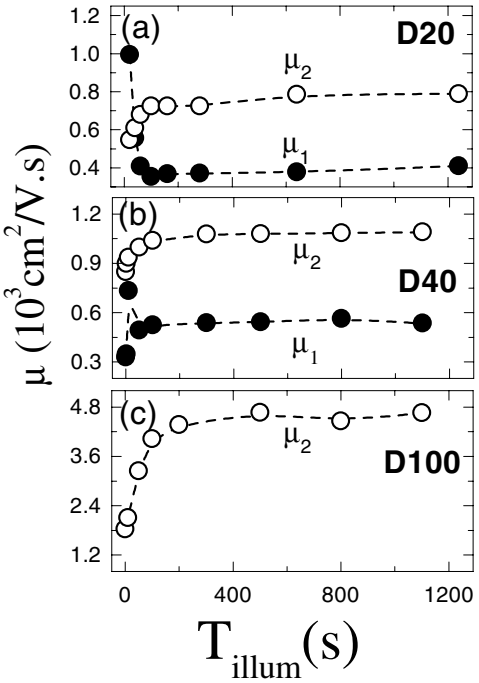

Figure 4. Quantum mobility of first and second subbands as a function of the illumination time for the samples: (a) D20; (b) D40 and (c) D100. The dashed lines connecting the peaks are a guide to the eyes.

at $T_{illum} = 20$ s are $\mu_1 = 995$ cm^2 V^{-1} s^{-1} and $\mu_2 = 546$ cm^2 V^{-1} s^{-1}, indicating that, at the beginning of the illumination process, the mobility of the first subband is larger than the one of the second subband. For sample D40, while the quantum mobility of the second subband monotonically increases with the illumination time, the mobility of the first subband increases at the beginning of the illumination process ($0 \leqslant T_{illum} \leqslant 10$ s), has its value reduced at $T_{illum} = 50$ s and, from this moment onwards, turns to increase at a slower rate than before. For sample D100, the quantum mobility of the observed subband monotonically increases with illumination time.

As demonstrated by theoretical calculations in δ-doped semiconductors [13], the quantum mobility of individual electronic subbands is strongly correlated with the amount of overlap between the subband envelope wavefunction ($\Psi_i(z)$) and the dopant distribution function ($g_I(z)$) describing the region where the donor atoms are placed. It was demonstrated that for each subband, a change in the envelope wavefunction overlap with the doped region is accompanied by an opposite change in the mobility: when $\int |\Psi_i(z)|^2 g_I(z)\,\mathrm{d}z$ increases, μ_i decreases, and vice versa. So, assuming that Coulomb scattering on the ionized donors in the δ-doped layer dominates the conduction process, the quantum mobility of each subband can be described by

$$(\mu_i^{-1}) \propto \int |\Psi_i(z)|^2 g_I(z)\,\mathrm{d}z = \frac{1}{W_I}\int_{-W_I/2}^{W_I/2} |\Psi_i(z)|^2\,\mathrm{d}z \tag{1}$$

if a rectangular function of width W_I is used to describe the spatial distribution of the ionized donors around the δ-doped layer, i.e.,

$$g_I(z) = \begin{cases} \dfrac{1}{W_I} & \text{if } |z| \leqslant \dfrac{W_I}{2} \\ 0 & \text{otherwise.} \end{cases} \tag{2}$$

In the present work, we used the phenomenological relation (1) and the electronic envelope wavefunctions corresponding to the confined states in the active region obtained by self-consistent calculations to describe the changes observed in the experimental quantum mobilities presented in figure 4. To evaluate the overlap integral we used $W_I = 20$ Å. The results of our theoretical simulations are presented in the next section.

4. Band structure and data analysis

In order to get a qualitative picture of how the different subbands in the InGaAs QW and in the δ-doped QW behave when the carrier density increases by illumination, we calculated the subband structure for the electrons by solving the Poisson and Schrödinger equations self-consistently within the effective-mass formalism. The exchange and correlation effects have not been included in the self-consistent calculation since they have negligible effect on the conduction band profile [14]. The input to the self-consistent calculations comprises parameters related to the InGaAs and GaAs materials (effective masses, dielectric constants, bandgaps) and to the Si δ-doped layer (Si-doping concentration and width of the delta layer). The $In_xGa_{1-x}As$ bandgap (E_g) and the electron effective mass were obtained from interpolation [15]. Other parameters used in the calculations are the conduction-band offset taken to be $V_C = 0.7\Delta E_g$, In composition $x = 0.15$, doping density $N_{Si} = 4.0 \times 10^{12}$ cm^{-2}, well width $L_w = 150$ Å and impurity spread $W_I = 20$ Å.

Following our earlier work [10], here we also attributed the extra electrons in the active region of the samples to the presence of deep centres within the structure that trap part of the conduction electrons and release them under illumination. So, in order to simulate the changes of the electronic structure of the active region in the presence of deep traps, we assumed that the GaAs layer is uniformly doped with deep traps with an energy level below the conduction band. For all samples, to simulate the condition at $T_{illum} = 0$ s, we assumed a deep trap concentration (N_{DT}) around 1.0×10^{16} cm^{-3}. This choice was dictated by the fact that the electrons of the 2DEG are initially captured by the deep centres in the GaAs layer and the active region is strongly uncompensated. During illumination, the amount of negative charge in the GaAs layer changes due to the neutralization of the deep traps. The decrease of the negative charge of the GaAs layer is compensated for by increasing the density of the 2DEG in the active region. To simulate the saturated stages of illumination ($T_{illum} > 1000$ s) for all samples, we assumed a p-type carbon background spread over the whole structure with concentration[5] equal to 5.0×10^{14} cm^{-3}. In this way, only a small number of carriers will be captured by the carbon impurities and the electrons previously captured by the deep traps are forced to return to the active region after the illumination. Moreover, because the Fermi level at the active region is not known *a priori*, the amount of charge transferred into surface states due to the pinning must be determined self-consistently. So, in our simulations, two parameters were changed in order to obtain the best agreement between the calculated and experimentally determined subband occupancies before the illumination of the samples: the position of the Fermi level pinning at the free surface (V_S) and the concentration of deep traps in the GaAs layer. Once the value of V_S at $T_{illum} = 0$ s had been determined, this value of V_S was also used to determine the electronic structure of the system in the saturated

[5] GaAs layer grown by MBE are always lightly p-type due to carbon incorporation and a background of 1×10^{15} cm^{-3} represents an upper limit of impurity concentration for samples grown by this technique.

Table 1. Subband occupancies (N_i), mean distance ($\langle z_i \rangle$) between the ith electron distribution function and the δ-doped layer, value of the overlap integral (Int_i) between the ith envelope wavefunctions and the dopant distribution function, and Fermi wavevector (k_F) determined by the self-consistent calculations.

Sample	Sub-band	T_{illum} (s)	N_i (10^{12} cm^{-2})	$\langle z_i \rangle$ (Å)	Int_i	k_F (10^6 cm^{-1})
	1	0	1.91	−33.4	0.15	3.46
	1	1240	2.32	−26.5	0.17	3.82
D20	2	0	0.74	−23.2	0.09	2.16
	2	1240	1.07	−23.4	0.07	2.59
	3	0	0.07	−15.2	0.02	0.66
	3	1240	0.33	−18.3	0.02	1.43
	1	0	1.71	−30.7	0.15	3.28
	1	1100	2.15	−17.5	0.21	3.68
D40	2	0	1.00	−32.6	0.08	2.46
	2	1100	1.28	−42.1	0.05	2.83
	3	0	0.10	−23.2	0.03	0.77
	3	1100	0.37	−14.6	0.03	1.53
	1	0	0.69	−19.3	0.18	2.08
	1	1100	1.32	+6.5	0.25	2.88
D100	2	0	0.51	−118.0	0.05	1.79
	2	1100	0.74	−139.4	0.01	2.16
	3	0	0.00	—	—	—
	3	1100	0.09	+34.1	0.03	0.75

stage of illumination. Assuming that the origin of the energy scale is at the Fermi energy, the best fit of the occupancies at $T_{illum} = 0$ s was obtained with $N_{DT} = 1.0 \times 10^{16}$ cm^{-3} and $V_S = 180$ meV for sample D20, and $N_{DT} = 1.0 \times 10^{16}$ cm^{-3} and $V_S = 250$ meV for sample D40. Because only one subband was observed in the SdH measurements of sample D100, we were not able to determine simultaneously the values of V_S and N_{DT}. Since the Fermi level seems to converge to the value $V_S = 250$ meV as we increase the thickness of the spacer layer, we adopted this value for sample D100. The best fit of the occupancies for sample D100 was obtained with $N_{DT} = 0.95 \times 10^{16}$ cm^{-3}. We also assumed in all simulations that the Fermi level is pinned in the middle gap of the GaAs bulk material in the semi-infinite region of the thick GaAs back barrier. In figures 5–7, the conduction band edge and the squared envelope functions ($\Phi_i = |\Psi_i(z)|^2$) for the first (Φ_1), second (Φ_2) and third (Φ_3) electron subbands are shown both at $T_{illum} = 0$ s and in the saturated stages of illumination for all the structures here investigated. Some results of the theoretical calculations which are important for the discussion of the data are presented in table 1. In this table are shown the theoretical values for the occupancies of the subbands (N_i), the value of the overlap integral (Int_i) between the ith envelope wavefunctions and the dopant distribution function, and the values of the Fermi wavevector (k_F). The integral describing the interaction of the electron wavefunction and the dopant distribution was calculated using a rectangular function of width $W_I = 20$ Å. We also show in this table the value of the mean distance ($\langle z_i \rangle$) between the ith electronic distribution function and the δ-doped layer at $z = 0$, estimated by $\langle z_i \rangle = \int_{-\infty}^{+\infty} \Psi_i^* z \Psi_i \, \mathrm{d}z$.

The theoretical results for sample D20 showed that the electronic distribution of the first subband (see figure 5), that was initially located in the InGaAs QW ($\langle z_1 \rangle = -33.4$ Å), moves towards the δ-doped layer under illumination ($\langle z_1 \rangle = -26.5$ Å), meaning that the average distance between the carriers in the fundamental state and the Si ionized donors of the delta

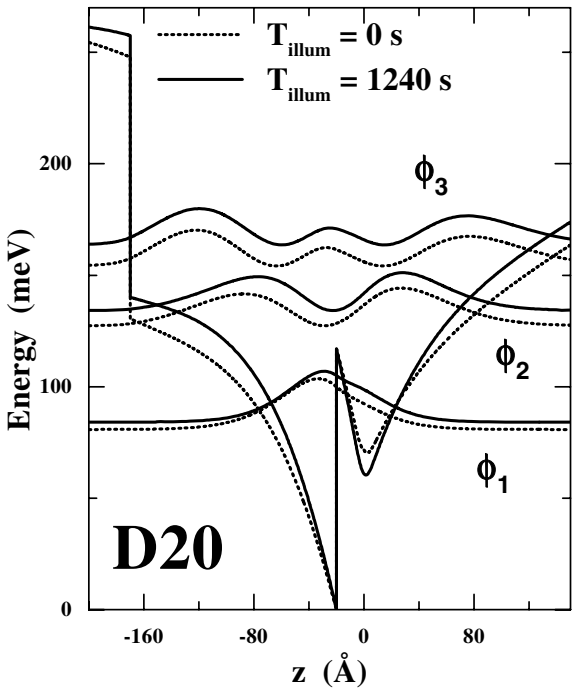

Figure 5. The conduction band edge in the vicinity of the active region and the squared envelope functions for the first (Φ_1), second (Φ_2) and third (Φ_3) subbands at $T_{illum} = 0$ s (dashed curves) and the saturated stage of illumination (solid curves) for sample D20. The δ-doped QW is centred at $z = 0$ and the InGaAs QW width is 150 Å.

layer decreases during the illumination process. The approximation of the electron distribution to the proximity of the δ-doped layer leads to an increase of $\sim$13% in the value of the overlap integral, yielding a reduction of the carrier mobility in this subband. The influence of the illumination on the electron distribution function related to the second subband does not change the average distance ($\langle z_2 \rangle = -23.2$ Å) of the distribution in relation to the δ-doped layer, but leads to a decrease of $\sim$22% in the value of the overlap integral, yielding an increase of the carrier mobility in this subband. As already explained in a previous work [10], computational artifacts did not allow us to compute the experimental quantum mobility of the third subband but the self-consistent calculations indicate that the mobility of this subband should increase with the illumination of the sample.

For sample D40, the overlap integral related to the first subband increases 40% with illumination, which should lead to a decrease of the carrier mobility in this subband, contrary to the experimental observation presented in figure 2. However, as we explain below, the overlap integral is not the unique parameter that needs to be taken into account in order to describe the behaviour of the carrier mobility in such a system. The relative electron mobility of each subband of a 2DEG has already been determined by several groups in δ-doped systems, and it always came out that its value was smaller in the fundamental electronic subband and increased with rising subband index [16–18]. In contrast, as mentioned above, work on conventional modulation-doped QWs showed that the mobility in the fundamental subband is higher than in the excited subbands [19–21].

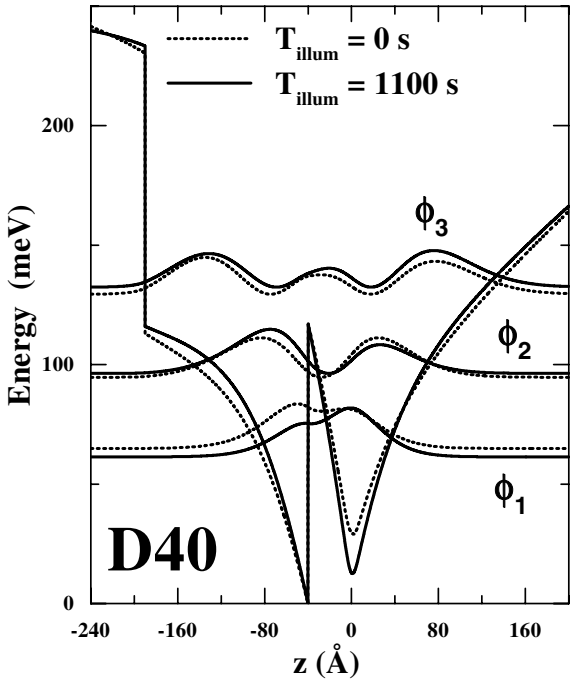

Figure 6. The conduction band edge in the vicinity of the active region and the squared envelope functions for the first (Φ_1), second (Φ_2) and third (Φ_3) subbands at $T_{illum} = 0$ s (dashed curves) and the saturated stage of illumination (solid curves) for sample D40. The δ-doped QW is centred at $z = 0$ and the InGaAs QW width is 150 Å.

These observations can be understood in terms of the interplay between

(i) the physical separation of the electron distribution from the ionized donors which gives reduced scattering as its separation from the ionized impurities in the δ-doped layer increases, and
(ii) the Fermi velocity of the carriers which is lower in the higher subbands, resulting in increasing scattering and, therefore, lower mobility.

As can be seen in figure 6, when the spacer thickness is 40 Å, the InGaAs QW and the δ-doped QW begin to be uncoupled: the electron wavefunction of the first subband has two well defined local maxima (one within each QW) but does not have any node. Once the maximum inside the InGaAs QW is far from ($\approx$50 Å) the plane of Si atoms and the other maximum is at the same position as the δ-doped layer, how should we analyse such a sample: as a typical delta-doped system in which the 2DEG is confined in a region close to the ionized donors, or a typical modulation-doped heterostructure in which the 2DEG is separated from the impurities by a wide spacer?

In fact, the behaviour of the mobility of the first subband of sample D40 is determined by a combination of these two mechanisms and can be described as follows: at the beginning of the illumination process ($0 \leqslant T_{illum} \leqslant 10$ s) the increase of the mobility is determined by the increase of the electronic Fermi velocity as a consequence of the large increase of the subband carrier density. Soon after, the movement of the electronic distribution towards the δ-doped layer and the increase of the overlap integral with the Si-donor distribution becomes significative leading to a decrease in the mobility at $T_{illum} = 50$ s. From this moment onwards, the mobility increases at a lower rate than before indicating that, even though the electronic

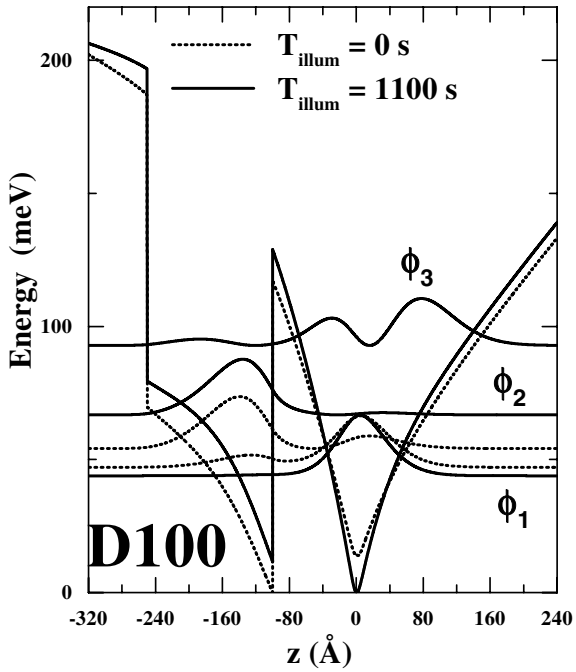

Figure 7. The conduction band edge in the vicinity of the active region and the squared envelope functions for the first (Φ_1), second (Φ_2) and third (Φ_3) subbands at $T_{illum} = 0$ s (dashed curves) and the saturated stage of illumination (solid curves) for sample D100. The δ-doped QW is centred at $z = 0$ and the InGaAs QW width is 150 Å.

function gets closer to the Si-ionized donors, the increase of the Fermi velocity determines the behaviour of the mobility during the whole illumination process. Differently from sample D40, the scattering by ionized impurities in the δ-doped layer is the effect which determines the behaviour of the mobility of the first subband of sample D20 instead of the increase of Fermi velocity of the carriers. For the second subband of sample D40, the theoretical results showed that the electronic distribution function (at a mean distance $\langle z_2 \rangle = -32.6$ Å at $T_{illum} = 0$ s) moves apart from the δ-doped layer, toward the InGaAs QW ($\langle z_2 \rangle = -42.1$ Å), during the illumination process. So, the increase of the separation of the electron distribution from the Si-ionized donors as well as the increase of the carrier Fermi velocity contributes to the increase of the mobility of the second subband with illumination. Although the calculations indicate a third occupied subband, we did not detect such a subband in our SdH measurements probably due to the small Fermi velocity of the electrons (very low occupation).

The theoretical simulations for sample D100 indicate that the InGaAs QW and the δ-doped QW are almost completely decoupled and there are two occupied subbands at $T_{illum} = 0$ s and three occupied subbands in the saturated stage of illumination. The analysis of the theoretical data indicates that only the oscillations related to the second subband were detected in our SdH measurements. As can be observed in figure 7, the electronic distribution function of the second subband is predominantly localized inside the InGaAs QW, which leads to carriers with high values of mobility. In contrast, the electronic distribution of the first subband is strongly localized in the δ-doped QW. For this reason, the oscillations related to the $i = 1$ subband were not detected in our SdH measurements. The wavefunction of the electrons in the third subband is spread over both QWs and its occupancy is very low. So, due to these two factors, the oscillations related to the third subband were not observed in the SdH measurements.

At $T_{illum} = 0$ s, the mean distance of the $i = 2$ subband from the Si-ionized donors is $\langle z_2 \rangle = -118.0$ Å, which results in the high value of mobility ($\mu_2 = 1023.2$ cm^2 V^{-1} s^{-1}) for the carriers in this subband. The mobility increases up to $\mu_2 = 3129.7$ cm^2 V^{-1} s^{-1} in the saturated stage of illumination when the electronic distribution moves to an even bigger distance from the δ-doped layer ($\langle z_2 \rangle = -139.4$ Å).

5. Conclusion

In this work, the subband electronic structure of δ-doped modulation QWs was investigated by SdH measurements as a function of the illumination time of the samples. Before the exposure of the heterostructures to any illumination time, we observed that a significant number of electrons was missing in the active region of all analysed structures. During the illumination process, carriers were released by illumination and injected into the active region of the samples, leading to strong modifications in the quantum mobility of the subbands. Based on self-consistent calculations in which the band structure modifications induced by the injection of carriers in the active layer were taken into account, the dominant mechanism which caused the changes in the subband quantum mobility with illumination was elucidated.

Acknowledgments

The authors would like to acknowledge the financial support of FAPESP (grant no 2000/08794-6) and CNPq.

References

[1] Ferry D K and Goodnick S M 1997 *Transport in Nanostructures* (Cambridge: Cambridge University Press)
[2] Nguyen L D, Radulescu D C, Foisy M C, Tasker P J and Eastman L F 1989 *IEEE Trans. Electron Devices* **36** 833
[3] Schubert E F 1996 *Delta Doping of Semiconductors* ed E F Schubert (Cambridge: Cambridge University Press) p 498
[4] Ando T, Fowler A B and Stern F 1982 *Rev. Mod. Phys.* **54** 437
[5] Pfeiffer L, West K W, Stormer H L and Baldwin K W 1989 *Appl. Phys. Lett.* **55** 1888
[6] van der Burgt M, Karavolas V C, Peeters F M, Singleton J, Nicholas R J, Herlach F, Harris J J, Van hove M and Borghs G 1995 *Phys. Rev.* B **52** 12218
[7] Lo Ikai, Kao M J, Hsu W C, Kuo K K, Chang Y C, Weng H M, Chiang J C and Tsay S F 1996 *Phys. Rev.* B **54** 4774
[8] Babinski A, Li G and Jagadish C 1997 *Appl. Phys. Lett.* **71** 1664
[9] Zervos M, Elliott M and Westwood D I 1999 *Appl. Phys. Lett.* **74** 2026
[10] Cavalheiro A, da Silva E C F, Takahashi E K, Quivy A A, Leite J R and Meneses E A 2002 *Phys. Rev.* B **65** 111
[11] Yamada S and Makimoto T 1990 *Appl. Phys. Lett.* **57** 1022
[12] Henriques A B 1994 *Phys. Rev.* B **50** 8658
[13] Henriques A B 1996 *Phys. Rev.* B **53** 16365
[14] Ke Mao-long, Westwood D, Williams R H and Godfrey M J 1995 *Phys. Rev.* B **51** 5038
[15] Reddy U K, Ji G, Henderson T, Huang D, Houdre R, Morkoc H and Litton C W 1989 *J. Vac. Sci. Technol.* B **7** 1106
[16] Skuras E, Kumar R, Williams R L, Stradling R A, Dmochowski J E, Johnson E A, Mackinnon A, Harris J J, Beall R B, Skierbeszewski C, Singleton J, van der Wel P J and Wisniewski P 1991 *Semicond. Sci. Technol.* **6** 535
[17] Koenraad P M, van Hest B F A, Blom F A P, van Dalen R, Leys M, Perenboom J A A J and Wolter J H 1992 *Physica* B **177** 485
[18] Harris J J, Murray R and Foxon C T 1993 *Semicond. Sci. Technol.* **8** 31
[19] Gobsch G, Schulze D and Paasch G 1988 *Phys. Rev.* B **38** 10943
[20] van Houten H, Williamson J G, Broekart M E I, Foxon C T and Harris J J 1988 *Phys. Rev.* B **37** 2756
[21] Stormer H L, Gossard A C and Wiegmann W 1982 *Solid State Commun.* **41** 707